Liquid Crystals
Publication details, including instructions for authors and subscription information:
http://www.informaworld.com/smpp/title~content=t713926090

Transition metals complexed to ordered mesophases. XIII. Synthesis and mesomorphic properties of potentially ferroelectric Schiff's base palladium(II) complexes

M. Ghedini[a]; D. Pucci[a]; E. Cesarotti[b]; O. Francescangeli[c]; R. Bartolino[d]
[a] Dipartimento di Chimica, Università della Calabria, Arcavacata, CS, Italy [b] Dipartimento di Chimica Inorganica e Metallorganica ed Analitica, Centro CNR, Università di Milano, Milano, Italy [c] Dipartimento di Scienze dei Materiali e della Terra, Sezione Fisica Università di Ancona, Ancona, Italy [d] Dipartimento di Fisica, Università della Calabria, Arcavacata, CS, Italy

To cite this Article Ghedini, M. , Pucci, D. , Cesarotti, E. , Francescangeli, O. and Bartolino, R.(1993) 'Transition metals complexed to ordered mesophases. XIII. Synthesis and mesomorphic properties of potentially ferroelectric Schiff's base palladium(II) complexes', Liquid Crystals, 15: 3, 331 — 344

To link to this Article: DOI: 10.1080/02678299308029135

URL: http://dx.doi.org/10.1080/02678299308029135

LIQUID CRYSTALS, 1993, VOL. 15, NO. 3, 331–344

Transition metals complexed to ordered mesophases XIII†. Synthesis and mesomorphic properties of potentially ferroelectric Schiff's base palladium(II) complexes

by M. GHEDINI* and D. PUCCI
Dipartimento di Chimica, Università della Calabria,
I-87036 Arcavacata (CS), Italy

E. CESAROTTI
Dipartimento di Chimica Inorganica e Metallorganica ed Analitica, Centro CNR,
Università di Milano, Via Venezian 21, I-20133 Milano, Italy

O. FRANCESCANGELI
Dipartimento di Scienze dei Materiali e della Terra, Sezione Fisica Università di
Ancona, Via Brecce Bianche, I-60131 Ancona, Italy

and R. BARTOLINO
Dipartimento di Fisica, Università della Calabria,
I-87036 Arcavacata (CS), Italy

(*Received 2 November 1992; accepted 9 May 1993*)

A series of *N*-[4′-(dodecyloxy)resorcylidene]-4-(RO*)-anilines (HL_n $n=1$, R*O $=(-)$-*cis*-myrtanyl; $n=2$, R*O $=(-)$-menthyl; $n=3$, R*O = S-$(-)$-β-citronellyl; $n=4$, R*O = R-$(-)$-2-octyl) has been synthesized and the mesomorphic properties investigated. These ligands are able to chelate a metal atom; accordingly three different series of palladium complexes, [(Ln)Pd(Ln)], [(Ln)Pd(Azoxy-6)] and [(L_3)Pd(Ph-Py$_n$)] (where Azoxy-6 and PhPy$_n$ are cyclopalladated 4,4′-dihexyloxyazoxybenzene and 5-substituted-2-(4-substituted-phenyl)pyrimidine, respectively) have been prepared. The mesogenic HL_3 and HL_4 ligands exhibit a S_C^* phase, retained in [(L_3)Pd(L_3)], which changes to a cholesteric phase in [(L_4)Pd(L_4)] and becomes the more ordered S_H^* phase in the [(Ln)Pd(Azoxy-6)] ($n=3,4$) derivatives. In contrast, in the [(L_3)Pd(Ph-Py$_n$)] compounds the mesomorphic phase is a S_A phase.

1. Introduction

During the last few years, many efforts have been made to synthesize ferroelectric liquid crystal materials which exhibit chiral smectic C phases (S_C^*) suitable for electro-optic display devices.

Since the earlier attempts based on chiral benzylidene anilines [2–4], new interesting families of *N*-[4′-(alkoxy*)resorcylidene]-4-(alkyl)anilines [5–7] and *N*-[4′-(alkyl)resorcylidene]-4-(alkoxy*)anilines [8–9] have been described. Remarkably, the latter compounds are characterized by a high thermal stability and a wide smectic range, wherein the S_C^* phase occurs [10–12].

---

* Author for correspondence.

† For part XII see [1].

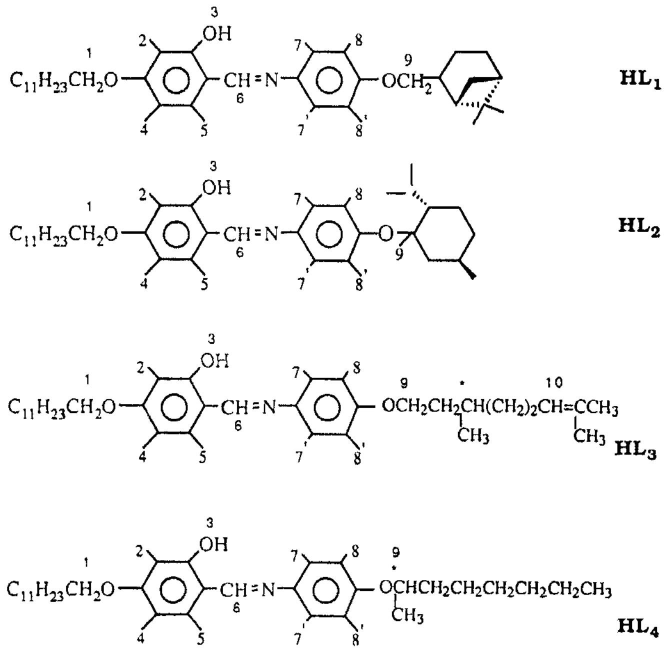

Figure 1. General formula of the HL_n Schiff's bases and proton numbering scheme.

We have recently described a new class of potentially ferroelectric metallomesogens derived by palladation of azoligands with chiral centres [1]. Now, with the aim of extending the investigations to other families of optically active compounds we have considered a homologous series of chiral Schiff's bases (**HL_n**, see figure 1), featuring a resorcylidene fragment able to chelate a transition metal atom. In the present paper we describe the synthesis, the mesomorphic properties and the X-ray diffraction characterization of the **HL_n** species and of three different series of mononuclear complexes, namely $[(L_n)Pd(L_n)]$, (**I–IV**), $[(L_n)Pd(\text{Azoxy-6})]$, (**V–VII**), and $[(L_3)Pd(\text{Ph-Py}_n)]$, (**IX–XII**), whose molecular structures include, together with a deprotonated **HL_n** ligand, a further **L_n** anion (**I–IV**), cyclometallated 4,4′-dihexyloxyazoxybenzene (azoxy-6, compounds **V–VIII**) or cyclometallated 5-substituted-2-(4-substituted-phenyl)pyrimidines (Ph-Py_n, compounds **IX–XII**).

2. Experimental

2.1. *Measurements*

^1H NMR spectra were recorded with Bruker WM-300 and AW 80 spectrometers using $CDCL_3$ solutions with Me_4Si as internal standard. Infrared spectra were obtained using a Perkin–Elmer 1330 spectrophotometer. Elemental analyses were performed by the Microanalysis Laboratory of the Dipartimento di Chimica, Università della Calabria, Italy.

The optical observations were made using a Zeiss Axioskop polarizing microscope coupled with a Linkam CO 600 heating stage equipped for photography. Transition temperatures and enthalpies were determined with a Perkin–Elmer DSC-7 differential scanning calorimeter, employing a heating/cooling rate of 10°C min^{-1}. The apparatus was calibrated using indium (156·6°C, 28·5 J g^{-1}). The X-ray powder diffraction patterns were obtained using an INEL CPS120 powder diffractometer equipped with a position sensitive detector covering a scattering angle of 120°, with an angular resolution of 0·018°. Monochromatic CuKα radiation ($\lambda = 1{\cdot}54$ Å) impinged on the sample which was ~1 mm thick and held at a temperature which was controlled to ±0·1°C by a hot stage containing electrical resistors.

2.2. *Synthesis*

The commercially available (−)-*cis*-myrtanol (1-S, 2-R)-6,6-dimethylbicyclo [3.1.1]hept-2-ylmethanol (99 per cent optical purity), (−)-menthol (1-R,2-S,5-R-2-isopropyl-5-methylcyclohexanol) (>99 per cent optical purity), S-(−)-β-citronellol (S-3,7-dimethyloct-6-en-l-ol) (>99 per cent optical purity), R-(−)-2-octanol (98 per cent optical purity) Fluka, A. G.), 4,4′-dihexyloxyazoxybenzene, (Eastman Kodak Co.), 5-substituted-2-(4-substituted-phenyl)pyrimidines (Merck, Darmstadt) and AgBF$_4$ (Fluka, A.G.) were used as received. [Pd(PhCN)$_2$Cl$_2$] [13], [Pd(azoxy-6)(MeCN)$_2$][BF$_4$] [14], [Pd(Ph-Py$_n$)(MeCN)$_2$][BF$_4$] [15, 16], 2-hydroxy-4-dodecyloxybenzladehyde [17], the chiral 4-nitroalkoxybenzenes [1] and 4-aminoalkoxybenzenes [1] were prepared according to the literature methods.

2.2.1. *Synthesis of the* ***HL$_n$*** *ligands*

In a typical procedure, equimolar amounts (1·6 mmol) of 2-hydroxy-4-dodecyloxybenzaldehyde and the appropriate 4-aminoalkoxybenzene were heated under reflux for 3·5 h in 10 ml of absolute ethanol. The reaction mixture was allowed to cool down (0°C) and the resulting precipitate was collected by filtration and washed with fresh ethanol. Colours, melting points, ^{1}H NMR data, elemental analysis results and yields for the compounds **HL$_n$** are given below:

HL$_1$: yellow solid, m.p. 82°C. ^{1}H NMR (80 MHz, CDCl$_3$) δ: 3·98 (m, 4 H, $H^{1,9}$), 6·44 (d, 1 H, H^4), 6·47 (s, 1 H, H^2), 6·90 (d, 2 H, $H^{8,8'}$), 7·21 (m, 3 H, $H^{5,7,7'}$), 8·49 (s, 1 H, H^6), 14·00 (s, 1 H, H^2). Elemental analysis (per cent): calcd. for $C_{35}H_{51}NO_3$: C, 78·75; H, 9·63; N, 2·62. Found: C, 79·06; H, 9·69; N, 2·62. Yield 90 per cent.

HL$_2$: yellow solid, m.p. 60°C. ^{1}H NMR (80 MHz, CDCl$_3$) δ: 3·97 (t, 3 H, $H^{1,9}$), 6·46 (m, 2 H, $H^{2,4}$), 6·92 (d, 2 H, $H^{8,8'}$), 7·21 (m, 3 H, $H^{5,7,7'}$), 8·48 (s, 1 H, H^6), 13·97 (s, 1 H, H^2). Elemental analysis (per cent) calcd. for $C_{35}H_{53}NO_3$: C, 78·46; H, 9·97; N, 2·61. Found: C, 78·33; H, 10·12; N, 2·60. Yield 64 per cent.

HL$_3$: yellow solid, thermotropic behaviour in table 1. ^{1}H NMR (80 MHz, CDCl$_3$) δ: 3·97 (m, 4 H, $H^{1,9}$), 5·11 (m, 1 H, H^{10}), 6·46 (m, 2 H, $H^{2,4}$), 6·91 (d, 2 H, $H^{8,8'}$), 7·21 (m, 3 H, $H^{5,7,7'}$), 8·48 (s, 1 H, H^6), 13·94 (s, 1 H, H^2). Elemental analysis (per cent): calcd. for $C_{35}H_{53}NO_3$: C, 78·46; H, 9·97; N, 2·61. Found: C, 78·36; H, 10·02; N, 2·56. Yield 77 per cent.

HL$_4$: yellow solid, thermotropic behaviour in table 1. ^{1}H NMR (80 MHz, CDCl$_3$) δ: 4·00 (t, 2 H, H^9), 4·37 (m, 1 H, H^1), 6·48 (m, 2 H, $H^{2,4}$), 6·93 (d, 2 H, $H^{8,8'}$), 7·24 (m, 3 H, $H^{5,7,7'}$), 8·51 (s, 1 H, H^6), 13·90 (s, 1 H, H^2). Elemental analysis (per cent): calcd. for $C_{33}H_{51}NO_3$: C, 77·75; H, 10·08; N, 2·75. Found: C, 77·77; H, 10·09; N, 2·83. Yield 90 per cent.

2.2.2. *Synthesis of* [(*L$_n$*)*Pd*[(*L$_n$*)] *complexes* (***I–IV***)

In a typical procedure, NaOH (0·56 mmol) in EtOH (1·05 ml) and solid Pd(PhCN)$_2$Cl$_2$ (0·27 mmol) were added to a solution of **HL$_n$** (0·56 mmol) in dioxane

(15 ml). The suspension was stirred for 30 min at room temperature: *n*-hexane (50 ml) was added and the mixture was cooled, filtered from a black residue and evaporated under reduced pressure leaving a solid product. This residue was crystallized from chloroform/ethanol (20/80, v/v). Colours, melting points, ^{1}H NMR data, elemental analysis results and yields for **I–IV** are given below:

$[L_1(Pd)L_1]$, **I**: yellow solid, m.p. 144°C. ^{1}H NMR (300 MHz, $CDCl_3$) δ: 3·79 (t, 2 H, H^1), 3·92 (m, 2 H, H^9), 5·66 (d, 1 H, H^2), 6·14 (dd, 1 H, H^4), 6·89 (dd, 2 H, $H^{8,8'}$), 7·01 (d, 1 H, H^5), 7·22 (dd, 2 H, $H^{7,7'}$), 7·55 (s, 1 H, H^6). Elemental analysis (per cent): calcd. for $C_{70}H_{100}N_2O_6Pd$: C, 71·74; H, 8·60; N, 2·39. Found: C, 71·95; H, 8·70; N, 1·82. Yield 76 per cent.

$[L_2(Pd)L_2]$, **II**: yellow solid, m.p. 115°C. ^{1}H NMR (300 MHz, $CDCl_3$) δ: 3·78 (t, 2 H, H^1), 4·05 (m, 1 H, H^9), 5·66 (d, 1 H, H^2), 6·14 (dd, 1 H, H^4), 6·91 (dd, 2 H, $H^{8,8'}$), 7·02 (d, 1 H, H^5), 7·22 (dd, 2 H, $H^{7,7'}$), 7·57 (s, 1 H, H^6). Elemental analysis (per cent): calcd. for $C_{70}H_{104}N_2O_6Pd$: C, 71·49; H, 8·91; N, 2·38. Found: C, 72·56; H, 9·10; N, 1·90. Yield 62 per cent.

$[L_3(Pd)L_3]$, **III**: yellow solid, thermotropic behaviour in table 2. ^{1}H NMR (300 MHz, $CDCl_3$) δ: 3·79 (t, 2 H, H^1 or H^9), 4·03 (t, 2 H, H^1 or H^9), 5·12 (m, 1 H, H^{10}), 5·65 (d, 1 H, H^2), 6·14 (dd, 1 H, H^4), 6·92 (dd, 2 H, $H^{8,8'}$), 7·02 (d, 1 H, H^5), 7·23 (dd, 2 H, $H^{7,7'}$), 7·56 (s, 1 H, H^6). Elemental analysis (per cent): calcd. for $C_{70}H_{104}N_2O_6Pd$: C, 71·49; H, 8·91; N, 2·38. Found: C, 70·83; H, 8·92; N, 2·12. Yield 75 per cent.

$[L_4(Pd)L_4]$, **IV**: yellow solid, thermotropic behaviour in table 2. ^{1}H NMR (300 MHz, $CDCl_3$) δ: 3·77 (t, 2 H, H^1), 4·36 (m, 1 H, H^9), 5·64 (d, 1 H, H^2), 6·14 (dd, 1 H, H^4), 6·89 (dd, 2 H, $H^{8,8'}$), 7·01 (d, 1 H, H^5), 7·21 (dd, 2 H, $H^{7,7'}$), 7·56 (s, 1 H, H^6). Elemental analysis (per cent): calcd. for $C_{66}H_{108}N_2O_6Pd$: C, 70·03; H, 9·62; N, 2·47. Found: C, 70·71; H, 9·01; N, 2·32. Yield 70 per cent.

2.2.3. *Synthesis of* $[(L_n)Pd(azoxy\text{-}6)]$ *complexes* (*V–VIII*)

In a typical procedure, the stoichiometric amount of $[Pd(azoxy\text{-}6)(MeCN)_2][BF_4]$ was added to a suspension of the HL_n ligand (0·4 mmol) in absolute ethanol (13 ml). The mixture was stirred for several hours (see below) at room temperature. The orange precipitate was filtered off and crystallized from chloroform/diethyl ether (20/80, v/v) to give the pure compounds. Colours, times of reaction, melting points, ^{1}H NMR data (*N,N-trans*-isomers), elemental analysis results and yields for **V–VIII** are given below:

$[L_1(Pd)azoxy\text{-}6]$, **V**: orange solid, 3 h, m.p. 120°C. ^{1}H NMR (300 MHz, $CDCl_3$) δ: 3·35 (t, 2 H, $-OCH_2$), 3·88 (t, 4 H, $-OCH_2$), 4·04 (t, 2 H, $-OCH_2$), 5·45 (d, 1 H, H^{12}), 5·92 (d, 1 H, H^2), 6·15 (dd, 1 H, H^4), 6·52 (dd, 1 H, H^{13}), 7·04 (d, 1 H, H^5), 7·46 (m, 1 H, H^4), 8·51 (s, 1 H, H^{14}), 7·84 (s, 1 H, H^6). Elemental analysis (per cent): calcd. for $C_{59}H_{83}N_3O_6Pd$: C, 68·35; H, 8·07; N, 4·05. Found: C, 68·08; H, 7·99; N, 4·12. Yield 75 per cent.

$[L_2(Pd)azoxy\text{-}6]$, **VI**: yellow solid, 15 h, m.p. 90°C. ^{1}H NMR (300 MHz, $CDCl_3$) δ: 3·38 (t, 2 H, $-OCH_2$), 3·89 (t, 2 H, $-OCH_2$), 4·04 (m, 3 H, $-OCH$ and $-OCH_2$), 5·52 (d, 1 H, H^{12}), 5·94 (d, 1 H, H^2), 6·16 (dd, 1 H, H^4), 6·52 (dd, 1 H, H^{13}), 7·05 (d, 1 H, H^5), 7·48 (m, 1 H, H^4), 7·85 (s, 1 H, H^6). Elemental analysis (per cent): calcd. for $C_{59}H_{85}N_3O_6Pd$: C, 68·22; H, 8·24; N, 4·04. Found: C, 68·10; H, 8·30; N, 3·90. Yield 60 per cent.

[L_3(Pd)azoxy-6], **VII**: orange solid, 5 h, thermotropic behaviour in table 3. ^{1}H NMR (300 MHz, $CDCl_3$) δ: 3·35 (t, 2 H, $-OCH_2$), 3·96 (m, 6 H, $-OCH_2$), 5·11 (m, 1 H, H^{10}), 5·44 (d, 1 H, H^{12}), 5·92 (d, 1 H, H^2), 6·15 (dd, 1 H, H^4), 6·52 (dd, 1 H, H^{13}), 7·04 (d, 1 H, H^5), 7·47 (m, 1 H, H^4), 7·84 (s, 1 H, H^6). Elemental analysis (per cent): calcd. for $C_{59}H_{85}N_3O_6Pd$: C, 68·22; H, 8·24; N, 4·04. Found: C, 68·30; H, 8·11; N, 4·20. Yield 70 per cent.

[L_4(Pd)azoxy-6], **VIII**: orange solid, 20 h, thermotropic behaviour in table 3. ^{1}H NMR (300 MHz, $CDCl_3$) δ: 3·37 (t, 2 H, $-OCH_2$), 3·88 (t, 2 H, $-OCH_2$), 4·03 (m, 3 H, $-OCH$ and $-OCH_2$), 5·48 (d, 1 H, H^{12}), 5·93 (d, 1 H, H^2), 6·15 (dd, 1 H, H^4), 6·51 (dd, 1 H, H^{13}), 7·04 (d, 1 H, H^5), 7·47 (m, 1 H, H^4), 7·85 (s, 1 H, H^6). Elemental analysis (per cent): calcd. for $C_{57}H_{83}N_3O_6Pd$: C, 67·60; H, 8·26; N, 4·15. Found: C, 67·86; H, 8·42; N, 4·12. Yield 90 per cent.

2.2.4. *Synthesis of* [(L_3)Pd(Ph-Py_n)] *complexes* (**IX–XII**)

In a typical procedure, a suspension of **HL_3** ligand (0·6 mmol) in absolute ethanol (10 ml) with the stoichiometric amount of the appropriate [Pd(Ph-Py_n)$(MeCN)_2$][BF_4] salt was stirred for a prolonged period (see below) at room temperature. The yellow precipitate formed was filtered off and crystallized from chloroform/ethanol (20/80, v/v) to give **IX–XII** as pure complexes. Colours, times of reaction, melting points, elemental analysis results and yields for **X–XII** are given below:

[(L_3)Pd(Ph-Py_1)], **IX**: yellow solid, 24 h, thermotropic behaviour in table 4. Elemental analysis (per cent): calcd. for $C_{52}H_{73}N_3O_4Pd$: C, 68·59; H, 8·08; N, 4·61. Found: C, 67·67; H, 7·91; N, 5·11. Yield 58 per cent.

[(L_3)Pd(Ph-Py_2)], **X**: yellow solid, 20 h, thermotropic behaviour in table 4. Elemental analysis (per cent): calcd. for $C_{62}H_{93}N_3O_4Pd$: C, 70·86; H, 8·92; N, 3·99. Found: C, 70·12; H, 8·79; N, 4·23. Yield 65 per cent.

[(L_3)Pd(Ph-Py_3)], **XI**: yellow solid, 4 d, thermotropic behaviour in table 4. Elemental analysis (per cent): calcd. for $C_{63}H_{95}N_3O_4Pd$: C, 71·06; H, 8·99; N, 3·95. Found: C, 71·28; H, 9·27; N, 3·97. Yield 62 per cent.

[(L_3)Pd(Ph-Py_4)], **XII**: yellow solid, 24 h, thermotropic behaviour in table 4. Elemental analysis (per cent): calcd. for $C_{55}H_{79}N_3O_4Pd$: C, 69·34; H, 8·36; N, 4·41. Found: C, 68·56; 8·07; N, 3·68. Yield 55 per cent.

3. Results and discussion

3.1. *HL_n ligands*

The optically active 4-aminoalkoxybenzene prepared from the readily available substances from the chiral pool of (−)-*cis*-myrtanol (1-S,2-R)-6,6-dimethylbicyclo [3.1.1] hept-2-ylmethanol, (−)-menthol (1-R,2-S,5-R-2-isopropyl-5-methylcyclohexanol), S-(−)-β-citronellol (S-3,7-dimethyloct-6-en-1-ol) or R-(−)-2-octanol [1], were condensed with 4-dodecyloxy-2-hydroxybenzaldehyde to give the corresponding chiral Schiff's bases, **HL_n** in good yields (see § 2).

The **HL_n** products are yellow solids, and amongst them **HL_3** and **HL_4**, derived from S-(−)-β-citronellol and R-(−)-2-octanol, respectively, show thermotropic mesomorphism (table 1). On the contrary, the ligands having a bulky, chiral group like (−)-*cis*-myrtanol (**HL_1**) and (−)-menthol (**HL_2**) were not liquid crystals.

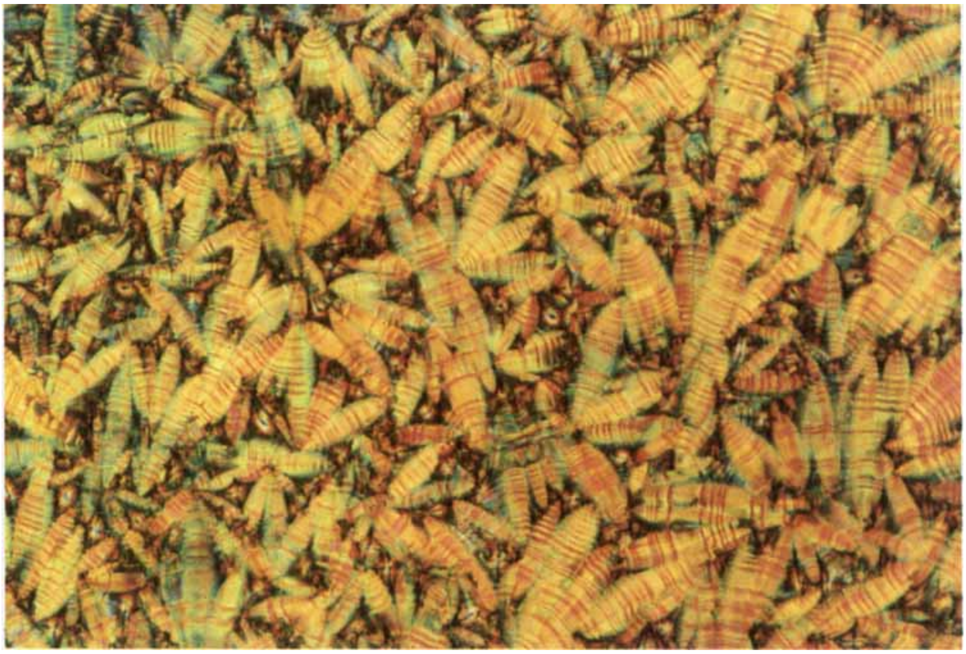

Figure 2. Optical micrograph showing the focal conic defect texture of the smectic C* phase in compound **HL$_3$** at 66°C (cooling cycle), × 200.

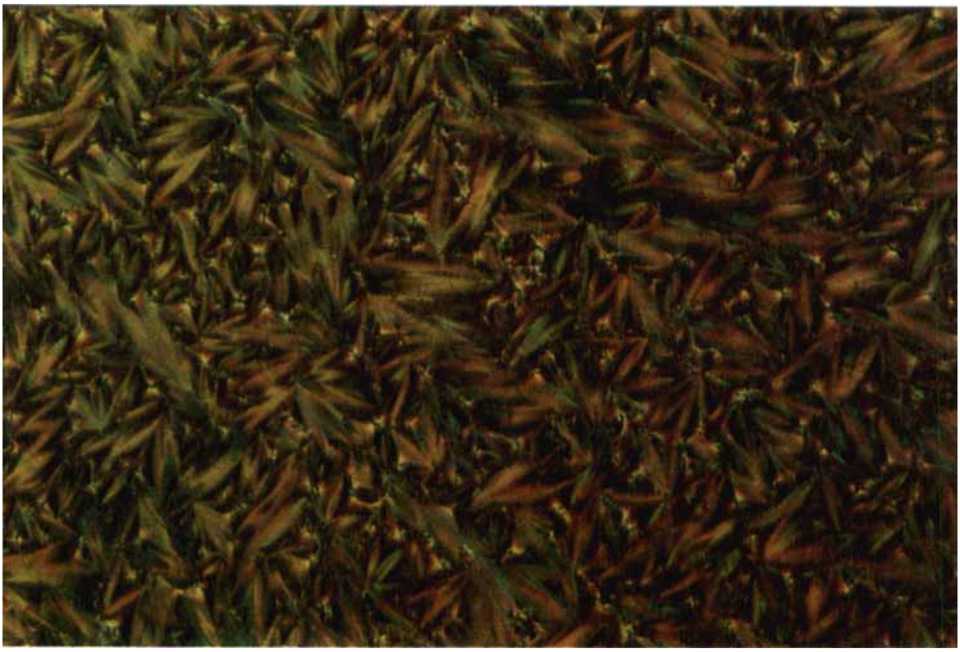

Figure 4. Optical micrograph showing the focal conic defect texture of the smectic C* phase in the complex **III** at 108°C (cooling cycle), × 200.

Table 1. Transition temperatures and enthalpy changes for the mesomorphic ligands HL_n†.

Compound	Transition	T/°C	ΔH/J g^{-1}	d/Å§	L/Å¶
HL_3	C–S_C^*	50·4	57·6	29·8	37·4
	S_C^*–I	77·3	14·0		
	I–S_C^*	74·3	14·2		
	S_C^*–C	44·0			
HL_4	C–S_C^*‡	47·0			
	S_C^*–I‡	48·0			
	I–S_C^*‡	48·0		30·8	36·2
	S_C^*–C‡	30·0			

† C, crystal; S, smectic; I, isotropic liquid.

‡ Transition observed only by optical microscopy.

§ Layer spacing derived from diffraction patterns (in the central region of the phases stability).

|| Molecular length determined by molecular modelling (alkyl chains in all *trans*-conformation).

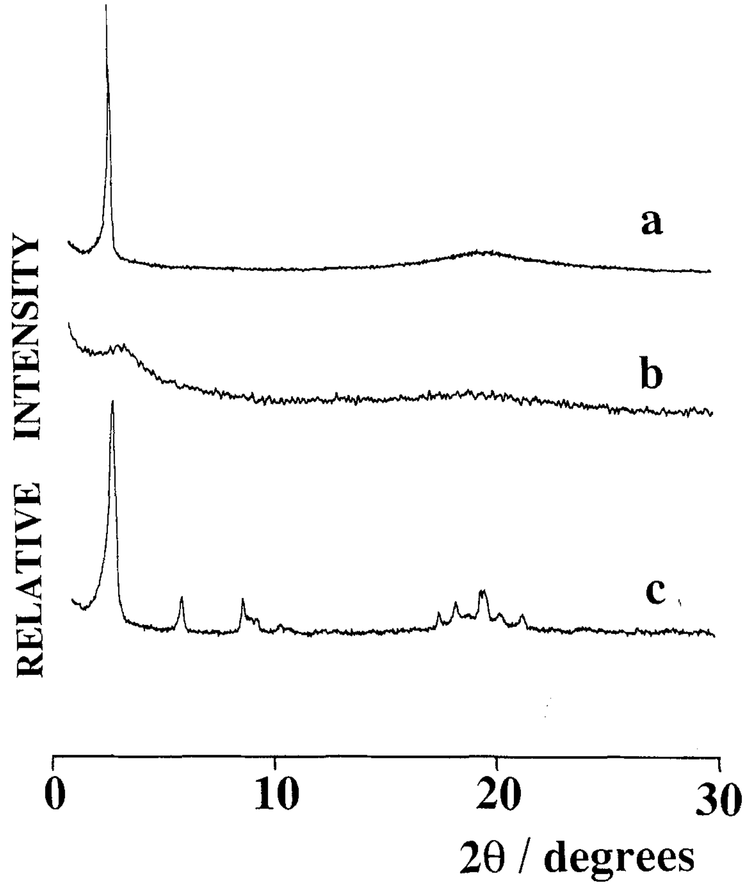

Figure 3. X-ray diffraction patterns for some of the investigated compounds, at different temperatures: (*a*) compound HL_3, $T = 64°C$ in the heating cycle; (*b*) compound **IV**, $T = 102°C$ in the cooling cycle; (*c*) compound **VIII**, $T = 130°C$ in the heating cycle.

As far as the mesomorphic properties are concerned, **HL$_3$** has a clearing point at about 77°C and forms an enantiotropic smectic C* phase (exhibiting the typical focal-conic defect texture, see figure 2), stable over a rather broad range of temperature (27°C). **HL$_4$** displays the same phase but this is stable over only a 1°C temperature range, before clearing at 48°C. Noticeably, on cooling down from the isotropic liquid, the **HL$_4$** S_C^* phase persists almost to room temperature (30°C).

In comparison with other *N*-[4′-(alkyl)resorcylidene]-4-(alkoxy*)anilines [8, 9], **HL$_3$** and **HL$_4$** show lower transition temperatures, a larger range of mesomorphism and are lacking S_A or cholesteric phases. However, with respect to the structurally similar *N*-[4′-(S)-(6-methyloctyloxy)resorcylidene]-4-(dodecyl)aniline [10], **HL$_4$** exhibits mesomorphic behaviour over a narrower range, with lower transition temperatures.

The values of the layer thickness, *d*, in the smectic phase have been obtained from the X-ray diffraction spectra and are reported in table 1. A comparison of these with the values of the molecular length in the fully extended configuration, *L*, (reported in table 1) allows us to estimate an upper limit of $\beta = 37°$ (**HL$_3$**) and $\beta = 32°$ (**HL$_4$**) for the average tilt angle β in the S_C^* phase. As an example, figure 3(*a*) reports the X-ray diffraction pattern measured for compound **HL$_3$**, at $T = 64°C$ on the heating cycle. Remarkably, in common for both compounds **HL$_3$** and **HL$_4$**, the shape of the X-ray diffraction peak in the low angle region of the spectrum is rather different for the two S_C^* phases obtained during, respectively, the heating and cooling cycles. In particular, the larger peak width measured on the cooling cycle reveals a considerably lower degree of correlation of the smectic layers for the corresponding phase.

3.2. [(L_n)Pd(L_n)] *complexes, I–IV*

The reaction between the chiral ligands **HL$_n$** and $Pd(PhCN)_2Cl_2$ (scheme I) affords the bis[*N*-4-(alkoxy)phenyl-4′-(dodecyloxy)salicylaldiminiatopalladium(II) complexes **I–IV** (see § 2). The phase sequence and transition temperatures for the complexes **I–IV** are summarized in table 2.

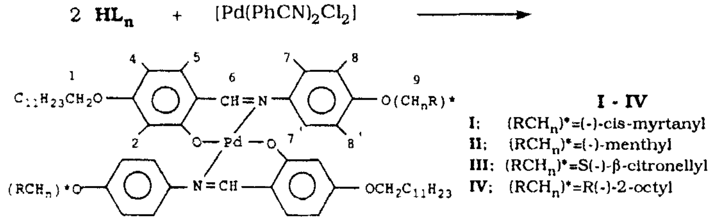

Scheme I. Synthesis and proton numbering scheme for the [(L_n)Pd(L_n)] complexes, I–IV.

The series **I–IV** behaves similarly to the parent **HL$_n$** series. In fact only the compounds containing S-(−)-β-citronellyl or R-(−)-2-octyl as the terminal chain, i.e. **III** and **IV**, show mesomorphism. In particular, on heating, compound **III** shows over a range of about 14°C a smectic A phase featured by its focal-conic texture. The clearing point is reached at 131°C. On cooling from the isotropic liquid however, the enantiotropic S_A phase persists only for 2°C, whereafter further cooling leads to a S_C^* phase having a striped fan-shaped texture (see figure 4). Following this unusual transitional behaviour, the S_C^* phase is present in the temperature range from 129°C to 90°C. In contrast, the mesomorphism of complex **IV** involves just a monotropic cholesteric phase stable over a very narrow range of temperature (about 1°C).

Table 2. Transition temperatures and enthalpy changes for the mesomorphic $[(L_n)Pd(L_n)]$ complexes†.

Compound	Transition	T/°C	ΔH/J g^{-1}	d/Å§	L/Å‖
$[(L_3)Pd(L_3)]$, **III**	C–S_A	117·3	35·3	32·0	37·4
	S_A–I	131·2	4·8		
	I–S_A‡	131·0			
	S_A–S_C^*	129·5	3·3		
	S_C^*–C	90·2	16·2		
$[(L_4)Pd(L_4)]$, **IV**	C–I	121·0	38·3		
	I–Ch	102·6	0·3	26·0	36·2
	Ch–C	101·5	4·9		

† C, crystal; S, smectic; Ch, cholesteric; I, isotropic liquid.

‡ Transition observed only by optical microscopy.

§ Layer spacing derived from diffraction patterns (in the central region of the phase's stability).

‖ Molecular length determined by molecular modelling (alkyl chains in all *trans*-conformation).

With reference to the corresponding uncomplexed ligands, the clearing points are raised by about 50°C in the case of complex **III** and 70°C in the case of **IV**; although it should be pointed out that the transition temperatures are considerably lower (about 70°C) than those reported for analogous achiral palladium(II) complexes [18].

The layer thickness in the S_A phase, d, measured from the X-ray diffraction pattern, is ~32 A°. Figure 3 (*b*) shows the X-ray spectrum recorded for compound **IV** for the cholesteric phase at $T = 102$°C. The corresponding d value reported in table 2 gives the 'apparent' molecular length as obtained by application of Bragg's law to the diffuse low angle peak.

3.3. $[(L_n)Pd(azoxy\text{-}6)]$ *complexes, V–VIII*

The addition of the chiral ligands HL_n to the cyclopalladated solvato species, $[Pd(azoxy\text{-}6)(MeCN)_2][BF_4]$ [scheme II) gives the $[(L_n)Pd(azoxy\text{-}6)]$ complexes, **V–VIII**. The identification of the complexes was carried out by elemental analysis and ^1H NMR (see § 2). Worthy of note, as previously observed for similar products [14, 19],

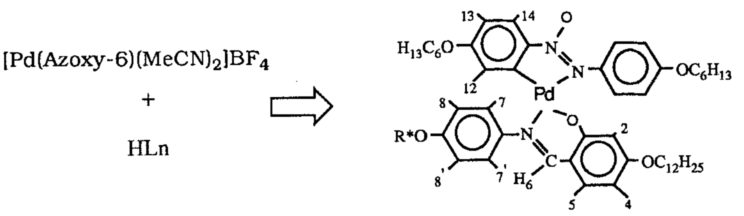

V-VIII

V; R*=(-)-cis-myrtanyl
VI; R*=(-)-menthyl
VII; R*=S(-)-β-citronellyl
VIII; R*=R(-)-2-octyl

Scheme II. Synthesis and proton numbering scheme for the $[(L_n)Pd(azoxy\text{-}6)]$ complexes, **V–VIII**.

Table 3. Transition temperatures and enthalpy changes for the [(L_n)Pd(azoxy-6)] complexes†.

Compound	Transition	T/°C	ΔH/J g^{-1}	d/Å‡	L/Å§
[(L_3)Pd(azoxy-6)], **VII**	C–S_H^*	107·2	1·2	30·2	37·4
	S_H^*–I	148·9	34·4		
	I–S_H^*	123·1	5·5		
	S_H^*–C	102·0	3·2		
	C–C_1	65·9	3·8		
[(L_4)Pd(azoxy-6)], **VIII**	C–S_H^*	113·0	33·1	29·2	36·2
	S_H^*–I	132·3	34·6		
	I–S_H^*	99·0	5·4		
	S_H^*–C	84·9	18·27		

† C, crystal; S, smectic; I, isotropic liquid.

‡ Layer spacing derived from diffraction patterns (in the central region of the phase's stability).

§ Molecular length determined by molecular modelling (alkyl chains in all *trans*-conformational).

the ^{1}H NMR spectra reveal the presence of two different signals for imine hydrogen, 0·05 ppm apart, accounted for by an isomeric mixture of *N*,*N*-*trans*-(depicted in scheme II) and *N*,*N*-*cis*-isomers in a *trans*-to *cis*-ratio of 9 to 1.

The mesomorphic behaviour of the [(L_n)(Pd(azoxy-6)] series, **V**–**VIII**, is summarized in table 3. Remarkably, the addition of the [Pd(azoxy-6)] fragment does change the mesomorphic properties of the **HL**$_n$ ligands. Indeed, complexes **VII** and **VIII** exhibit enantiotropic smectic phase, whereas no mesophase is observed for **V** or **VI**. The temperature range of the smectic phase in both cases is enhanced by about 20°C and the clearing points are raised by about 70°C with respect to the parent ligands **HL**$_3$ and **HL**$_4$.

The X-ray diffraction patterns for compound **VII**, measured at $T = 130$°C on the heating cycle, is shown in figure 3 (*c*). A similar behaviour is observed for **VIII**. Three diffraction peaks, corresponding to the first three orders of reflection from the smectic layers, are present in the low angle region and a set of discrete diffraction peaks, even if of low intensity, seems to be superimposed on the broad diffuse high angle halo. This is particularly evident in the spectrum of compound **VII**, while for compound **VIII**, the discrete peaks are much less well defined. This feature would suggest the presence of a certain degree of long range positional correlation within the smectic layers, which is consistent with the layered structure of an S_H^* phase, as indicated by optical observations.

Therefore, by comparing complexes **VII** and **VIII** with the compounds having similar molecular lengths and derived from achiral Schiff's bases, i.e. [*N*-(4′-hexyl or -octyl)phenyl)-2-(4-dodecyloxysalicylideneaminato] [4′(hexyloxyphenyl-NNO-azoxy-N^2-4-hexyloxyphenyl-2-ato]palladium (II) [14], it seems that the presence of an optically active centre induces a change in the smectic phase from S_A to S_H^* and a decrease in the melting points, whereas the clearing point remains substantially unchanged.

3.4. [(L_3)*Pd*(*Ph-Py*$_n$)] *complexes*, ***IX–XII***

The above reported data show that, as regards mesomorphic properties, the best results are obtained for the materials derived from **HL**$_3$. Thus such a ligand solely has reacted with the salts containing the solvato cyclopalladated phenylpyrimidine cations, i.e. $[Pd(Ph\text{-}Py_n)(MeCN)_2]BF_4$ (scheme III). The elemental analyses for the resulting products, **IX–XII**, confirms the $[(L_3)Pd(Ph\text{-}Py_n)]$ stoichiometry. The ^1H NMR spectra show, in the spectral region of aromatic protons, several signals that

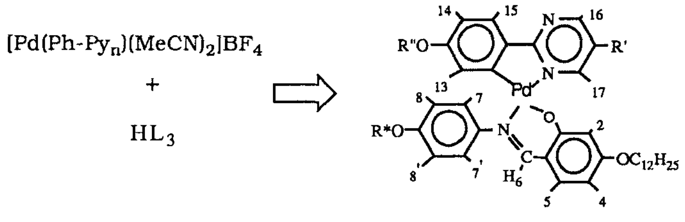

IX-XII

IX; $R'=C_6H_{13}$, $R''=CH_3$
X; $R'=C_9H_{19}$, $R''=CH_3$
XI; $R'=C_6H_{13}$, $R''=C_{11}H_{23}$
XII; $R'=C_9H_{19}$, $R''=C_9H_{19}$
R*= S(-)-β-citronellyl

Scheme III. Synthesis and proton numbering scheme for the $[(L_3)Pd(Ph\text{-}Py_n)]$ complexes, IX–XII.

Table 4. Transition temperatures and enthalpy changes for the mesomorphic complexes $[(L_n)Pd(Ph\text{-}Py_n)]$†.

Compound	Transition	$T/°C$	$\Delta H/J\,g^{-1}$	$d/Å$§	$L/Å$‖
$[(L_3)Pd(Ph\text{-}Py_1)]$, **IX**	$C\text{–}C_1$	86·9	20·1		
	$C_1\text{–}C_2$	92·6	11·3		
	$C_2\text{–}S_A$	105·3	11·3	27·6	37·4
	$S_A\text{–}I$	115·1	5·7		
	$I\text{–}S_A$	111·5	5·9		
	$S_A\text{–}C$‡	50·0			
$[L_3)Pd(Ph\text{-}Py_2)]$, **X**	$C\text{–}S_A$	103·6	6·1	30·4	37·4
	$S_A\text{–}I$	118·1	5·6		
	$I\text{–}S_A$	117·1	5·9		
	$S_A\text{–}C$‡	67·0			
$[(L_3)Pd(Ph\text{-}Py_3)]$, **XI**	$C\text{–}C_1$	103·4	9·8		
	$C_1\text{–}S_A$	112·6	15·5	30·2	37·4
	$S_A\text{–}I$	118·3	5·3		
	$I\text{–}S_A$	118·2	5·9		
	$S_A\text{–}C$‡	85·0			
$[(L_3)Pd(Ph\text{-}Py_4)]$, **XII**	$C\text{–}S_A$	97·7	0·6	28·4	37·4
	$S_A\text{–}I$	130·2	6·7		
	$I\text{–}S_A$	129·7	7·1		
	$S_A\text{–}C$‡	70·0			

† C, crystal; when two different solid phases are detected, C_1 indicates the solid phase stable over the lowest temperature range; S, smectic; I, isotropic liquid.

‡ Transition observed only by optical microscopy.

§ Layer spacing derived from diffraction patterns (in the central region of the phase's stability).

‖ Molecular length determined by molecular modelling (alkyl chains in all *trans*-conformation).

make it very hard to propose assignments. However, for **X**, a multiplet corresponding to a hydrogen and clearly attributable to H^{13} (scheme III) is detectable. Such a signal, $\delta = 5{\cdot}52$, is very close to the values ($\delta = 5{\cdot}44$–$5{\cdot}52$) obtained for the similar proton (H^{12} in scheme II) in the *N*,*N*-*trans*-isomers of **V–VIII**. Therefore we suggest that for **X** and, by analogy, for the whole [$(L_3)Pd(Ph\text{-}Py_n)$] series, that only the *N*,*N*-*trans*-complexes (depicted in scheme III) are formed.

All the compounds **IX–XII** are mesomorphic (table 4) as they exhibit at least a S_A phase (focal-conical fan texture) and also, for **IX** and **XI**, C–C_1, crystal–crystal changes. The clearing points of complexes **IX–XII** are higher, about 40°C on average, than those of the HL_n ligands, while the mesomorphic ranges are almost the same.

As an example of the X-ray diffraction results for the series of complexes **IX–XII**, figure 5 reports some X-ray spectra measured for compound **IX** at different

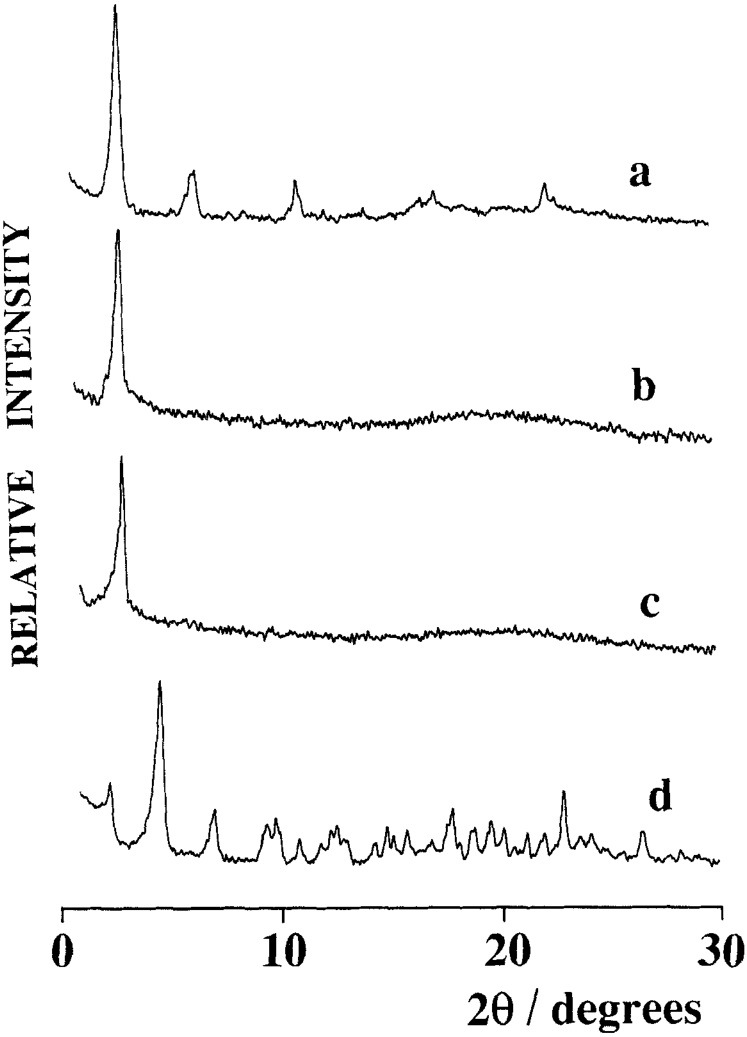

Figure 5. X-ray diffraction patterns of compound **IX** measured at different temperatures: (*a*) room temperature; (*b*) $T = 110°C$ in the heating cycle; (*c*) $T = 100°C$ in the cooling cycle; (*d*) room temperature, after a complete thermal cycle.

temperatures during a complete thermal cycle. The X-ray patterns in the S_A phase are very similar for all the compounds, with a narrow diffraction peak in the low angle region, which indicates a relatively high correlation of the smectic layers.

The values of the layer thickness in the smectic A phase range between 27·2 Å for compound **IX** and 30·4 Å for compound **X**. Therefore, with reference to this mesophase for **IX–XII** and for **III** as well, further investigations are necessary before proposing a complete model of the molecular packing; the considerable difference observed between the *d* and *L* values (tables 2 and 4) could be accounted for either by interdigitation or by a partial melting and folding of aliphatic chains, as already proposed for structurally similar mono-metallic mesogens [20].

In conclusion, this work has been devoted to the synthesis of new chiral mononuclear palladium mesogens incorporating a chiral fragment (i.e. (−)-*cis*-myrtanyl, (−)-menthyl, S-(−)-β-citronellyl, R-(−)-2-octyl) as alkoxy substituents (R*O) in a resorcylideneaniline structure. Several complexes displaying mesophases (Ch, S_A, S_C^*, S_H^*) have been prepared for R*O = S-(−)-β-citronellyl and R-(−)-2-octyl. Therefore the results parallel those recently reported for di-nuclear cyclopalladated chiral azobenzenes [1].

This work was financed by the Italian Consiglio Nazionale delle Ricerche (CNR) under the auspices of 'Progetto Finalizzato Materiali Speciali per Tecnologie Avanzate' and Ministero dell'Università e della Ricerca Scientifica e Tecnologica (MURST). We are grateful to Dr F. Neve for NMR measurements and for many helpful discussions. We also thank Johnson Matthey Research Centre, England, for a generous supply of $PdCl_2$.

References

[1] Ghedini, M., Pucci, D., Cesarotti, E., Antogniazza, P., Francescangeli, O., and Bartolino, R., 1993, *Chem. Mater.*, **5,** 883.

[2] Ostrovskii, B. I., Rabinovich, A. Z., Sonin, A. S., Sorkin, E. L., Strukov, B. A., and Taraskin, S. A., 1980, *Ferroelectrics*, **24,** 309.

[3] Hallsby, A., Nilsson, M., and Otterholm, B., 1982, *Molec. Crystals liq. Crystals Lett.*, **82,** 61.

[4] Billard, J., Dahlgren, A. Flatischler, K., Lagerwall, S. T., and Otterholm, B., 1986, *Molec. Crystals liq. Crystals*, **135,** 265.

[5] Barbera, J., Meléndez, E., Serrano, J. L., Sierra, M. T., Ezcurra, A., and Perez-Jubindo, M. A., 1989, *Molec. Crystals liq. Crystals*, **170,** 151.

[6] Sierra, T., Meléndez, E., Serrano, J. L., Ezcurra, A., and Perez-Jubindo, M. A., 1991, *Chem. Mater.*, **3,** 65.

[7] Meyer, R. B., Liebert, L., Strzelecki, L., and Keller, P., 1975, *J. Phys. Lett., Paris*, **36,** 69.

[8] Keller, P., Liebert, L., and Strzelecki, L., 1976, *J. Phys. Colloque C3*, **37,** 27.

[9] Keller, P., Juge, S., Liebert, L., and Strzelecki, L., 1976, *C. r. hebd. Séanc. Acad. Sci., Paris C*. **282,** 639.

[10] Otterholm, B., Nilsson, M., Lagerwall, S. T., and Skarp, K., 1987, *Liq. Crystals*, **2,** 757.

[11] Elguero, J., Jaime, C., Marcos, M., Meléndez, E., Sanchez-Ferrando, F., and Serrano, J. L., 1987, *Molec. Struct. (Theochem)*, **150,** 1.

[12] Gray, G. W., and Jones, B., 1955, *J. chem. Soc.*, p. 236.

[13] Karash, M. S., Seyber, R. C., and Mayo, F. R., *J. Am. chem. Soc.*, **60,** 882.

[14] Ghedini, M., Morrone, S., Francescangeli, O., and Bartolino, R., 1992, *Chem. Mater.*, **4,** 1119.

[15] Ghedini, M., and Pucci, D., 1990, *J. organomet. Chem.*, **395,** 105.

[16] Ghedini, M., Pucci, D., De Munno, G., Viterbo, D., Neve, F., and Armentano, S., 1991, *Chem, Mater.*, **3,** 67.

[17] Ghedini, M., Morrone, S., Gatteschi, D., and Zanchini, C., 1991, *Chem. Mater.*, **3,** 752.

[18] Caruso, U., Roviello, A., and Sirigu, A., 1988, *Liq. Crystals*, **3,** 1515.

[19] Ghedini, M., Morrone, S., De Munno, G., and Crispini, A., 1991, *J. organomet. Chem.*, **415,** 281.

[20] Bartolino, R., Rustichelli, F., Scaramuzza, N., Versace, C., M. C., Armentano, S., Ricci, M. A., Benassi, P., 1991, *Solid St. Commun.*, **80,** 587 and references therein.